Electrical control of antiferromagnetic domains in multiferroic $BiFeO_3$ films at room temperature

T. ZHAO[1]*†, A. SCHOLL[2]‡, F. ZAVALICHE[1]‡, K. LEE[1], M. BARRY[1], A. DORAN[2], M. P. CRUZ[1,3], Y. H. CHU[1], C. EDERER[4], N. A. SPALDIN[4], R. R. DAS[5], D. M. KIM[5], S. H. BAEK[5], C. B. EOM[5] AND R. RAMESH[1]†

[1]Department of Physics and Department of Materials Science and Engineering, University of California, Berkeley, California 94720, USA
[2]Advanced Light Source, Lawrence Berkeley National Lab, Berkeley, California 94720, USA
[3]Centro de Ciencias de la Materia Condensada (CCMC)-UNAM Km 107, Carretera Tijuana-Ensenada Ensenada B.C., C.P 22800, Mexico
[4]Materials Department, University of California, Santa Barbara, California 93106, USA
[5]Department of Materials Science and Engineering, University of Wisconsin, Madison, Wisconsin 53706, USA
*Present address: Seagate Research, 1251 Waterfront Place, Pittsburgh, Pennsylvania 15222, USA
‡These authors contributed equally to this work
†e-mail: tong.zhao@seagate.com; rramesh@berkeley.edu

Published online: 3 September 2006; doi:10.1038/nmat1731

Multiferroic materials, which offer the possibility of manipulating the magnetic state by an electric field or vice versa, are of great current interest. In this work, we demonstrate the first observation of electrical control of antiferromagnetic domain structure in a single-phase multiferroic material at room temperature. High-resolution images of both antiferromagnetic and ferroelectric domain structures of (001)-oriented multiferroic $BiFeO_3$ films revealed a clear domain correlation, indicating a strong coupling between the two types of order. The ferroelectric structure was measured using piezo force microscopy, whereas X-ray photoemission electron microscopy as well as its temperature dependence was used to detect the antiferromagnetic configuration. Antiferromagnetic domain switching induced by ferroelectric polarization switching was observed, in agreement with theoretical predictions.

Magnetoelectric coupling in multiferroic materials has attracted much attention because of the intriguing science underpinning this phenomenon and the exciting application potential in multiply controlled devices[1–7]. Several composite materials, consisting of separate piezoelectric and magnetic phases, have been reported to show magnetoelectric coupling at room temperature[8,9], a requirement for device applications. However, the availability of room-temperature single-phase multiferroics is very limited[10]. Among the few room-temperature single-phase magnetoelectric multiferroics reported so far[11], $BiFeO_3$ shows the highest ferroelectric polarization, with a ferroelectric Curie temperature (T_C) of ~1,100 K and an antiferromagnetic Néel temperature (T_N) of ~640 K. Both ferroelectricity and antiferromagnetism have long been known in $BiFeO_3$ single crystals[12–14], and recent studies of $BiFeO_3$ thin films[15–20] have confirmed the existence of a large ferroelectric polarization, as well as a small magnetization, both of which are consistent with theoretical predictions[21,22]. Although the possibility of coupling between the ferroelectric polarization and the weak ferromagnetism has been investigated using first-principles density functional theory[21], there have been no previous investigations of the coupling between ferroelectricity and antiferromagnetism in this material. In addition to its fundamental interest, such a coupling would offer the intriguing possibility of electric-field controllable ferromagnetism through exchange bias to an electrically controllable antiferromagnetic component.

In this work, we image the antiferromagnetic domain structure of $BiFeO_3$ films and record the changes induced in the antiferromagnetic domains on switching of the ferroelectric polarization. We use 600-nm-thick $BiFeO_3$ films, deposited on a

Report Documentation Page

Form Approved
OMB No. 0704-0188

1. REPORT DATE	2. REPORT TYPE	3. DATES COVERED
OCT 2006		**00-00-2006 to 00-00-2006**

4. TITLE AND SUBTITLE	5a. CONTRACT NUMBER
Electrical control of antiferromagnetic domains in multiferroic BiFeO3 films at room temperature	5b. GRANT NUMBER
	5c. PROGRAM ELEMENT NUMBER
6. AUTHOR(S)	5d. PROJECT NUMBER
	5e. TASK NUMBER
	5f. WORK UNIT NUMBER
7. PERFORMING ORGANIZATION NAME(S) AND ADDRESS(ES) **University of Wisconsin-Madison,Department of Materials Science and Engineering,Madison,WI,53706**	8. PERFORMING ORGANIZATION REPORT NUMBER
9. SPONSORING/MONITORING AGENCY NAME(S) AND ADDRESS(ES)	10. SPONSOR/MONITOR'S ACRONYM(S)
	11. SPONSOR/MONITOR'S REPORT NUMBER(S)

12. DISTRIBUTION/AVAILABILITY STATEMENT
Approved for public release; distribution unlimited

13. SUPPLEMENTARY NOTES

14. ABSTRACT

15. SUBJECT TERMS

16. SECURITY CLASSIFICATION OF:			17. LIMITATION OF ABSTRACT	18. NUMBER OF PAGES	19a. NAME OF RESPONSIBLE PERSON
a. REPORT	b. ABSTRACT	c. THIS PAGE			
unclassified	**unclassified**	**unclassified**	**Same as Report (SAR)**	**7**	

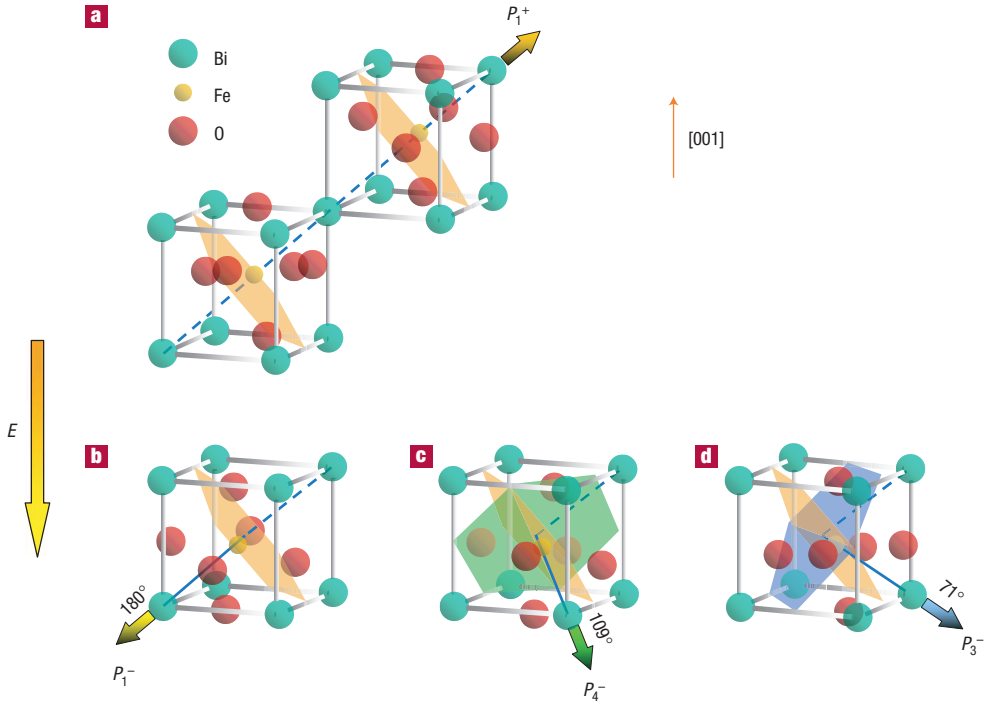

Figure 1 Schematic diagram of (001)-oriented $BiFeO_3$ crystal structure and the ferroelectric polarization (bold arrows) and antiferromagnetic plane (shaded planes). a, Polarization with an up out-of-plane component before electrical poling. **b**, 180° polarization switching mechanism with the out-of-plane component switched down by an external electrical field. The antiferromagnetic plane does not change with the 180° ferroelectric polarization switching. **c**,**d**, 109° (**c**) and 71° (**d**) polarization switching mechanisms, with the out-of-plane component switched down by an external electrical field. The antiferromagnetic plane changes from the orange plane to the green and blue planes on 109° and 71° polarization switching respectively.

conducting $SrRuO_3$ bottom electrode on $SrTiO_3$ (100) substrates by off-axis sputtering and pulsed laser deposition, as our model system. Ferroelectric measurements confirm a large polarization value of 55–60 $\mu C\,cm^{-2}$ along the surface normal, corresponding to a spontaneous polarization of 90–95 $\mu C\,cm^{-2}$ along the [111] directions of the rhombohedral unit cell. Magnetic measurements show a weak, saturated magnetic moment of 8–10 e.m.u. cm^{-3}, which is consistent with the magnitude of the canting of the antiferromagnetic sublattices calculated for $BiFeO_3$ in the absence of the long-wavelength spin spiral observed in bulk single crystals[21]. The ferroelectric domain structure is both imaged and switched using piezoelectric force microscopy (PFM). The antiferromagnetic domain structure is studied before and after electrical poling using photoemission electron microscopy (PEEM) based on X-ray linear dichroism (XLD)[23,24] at beamline 7.3.1.1 of the Advanced Light Source. We observe antiferromagnetic domain patterns which correlate clearly with the ferroelectric domains, as well as electrical-poling-induced antiferromagnetic domain switching; this is the first demonstration of magnetoelectric switching in a single-phase material at room temperature.

Bulk $BiFeO_3$ is a room-temperature ferroelectric with a spontaneous electric polarization directed along one of the [111] axes of the perovskite structure[12,14] (Fig. 1a). The ferroelectric and accompanying distortions reduce the symmetry from cubic to rhombohedral, and therefore the ferroelectricity is accompanied by a ferroelastic strain resulting from the distortion of the lattice. The ferroelectric polarization in $BiFeO_3$ can have eight possible orientations, corresponding to positive and negative orientation along the four cube diagonals, and the direction of the polarization can be switched by 180°, 109° and 71°: see Fig. 1b,c and d respectively. (Note that by 'switching' we mean reorientation of the polarization to a stable state that remains after the field is removed.) Switching of the polarization by either 109° or 71° changes the rhombohedral axis of the system and is therefore accompanied by a switching of the ferroelastic domain state.

The antiferromagnetic ordering is G-type; that is nearest-neighbour Fe moments are aligned antiparallel to each other in all three cartesian directions[13]. In bulk $BiFeO_3$, the orientation of the antiferromagnetic vector follows a long-wavelength spiral, which is believed to be suppressed in thin films[25]. Our earlier first-principles calculations of the magnetocrystalline anisotropy energy showed that the preferred orientation of the individual spins, in the absence of the spiral, is perpendicular to the rhombohedral axis[21]. Within the corresponding (111) plane there is a sixfold degeneracy, resulting in an effective 'easy magnetization plane' for the orientation of the magnetic moments. The orientation of the antiferromagnetic sublattice magnetization therefore seems to be coupled to the ferroelastic strain state of the system and should always be perpendicular to the ferroelectric polarization. As a result, polarization switching by either 71° or 109° should change the orientation of the easy magnetization plane. For example, if the polarization is switched by 109° from the [111] into the $[1\bar{1}\bar{1}]$ direction, the easy magnetization plane should change as indicated in Fig. 1c. (Figure 1d shows the analogous case of 71° switching.) Therefore, it follows that ferroelectric switching should lead to a reorientation of the antiferromagnetic order and that interesting magnetoelectric switching effects can be expected to occur in $BiFeO_3$ films.

All three types of ferroelectric polarization switching were observed in our previous PFM study of epitaxial thin films

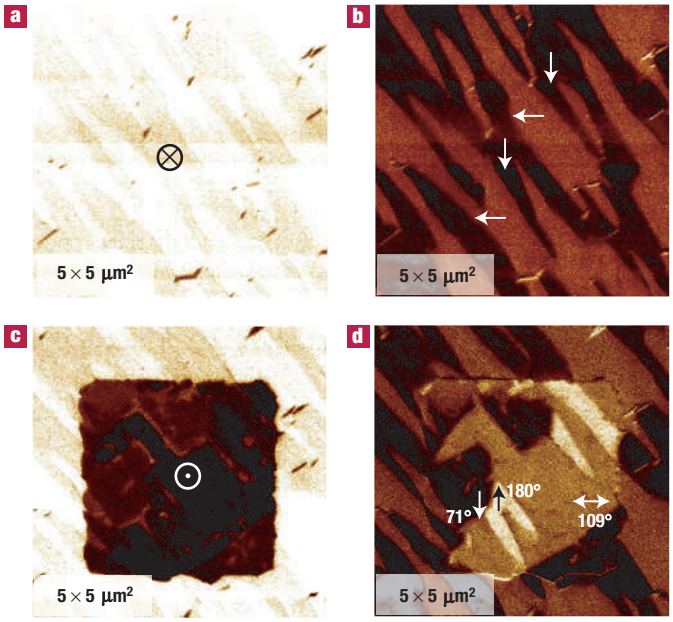

Figure 2 PFM images showing polarization domain structures of (001)-oriented $BiFeO_3$ film. a,**b**, Out-of-plane (**a**) and in-plane (**b**) PFM images of the as-grown film. ⊗ and the arrows represent the directions of out-of-plane and in-plane ferroelectric polarization components, respectively. **c**,**d**, Out-of-plane (**c**) and in-plane (**d**) PFM images taken after applying an electric field perpendicular to the film on the same area as in **a** and **b**. ⊙ indicates that the out-of-plane polarization component was switched by the applied electric field. The arrows in **d** indicate new in-plane polarization directions after ferroelectric switching. Different polarization switching mechanisms are labelled in **d**.

deposited on a (001)-oriented substrate[26,27], as shown in Fig. 2. In this work, we study the effects of these switching processes on the antiferromagnetic order, to verify the theoretical predictions outlined in the previous paragraph. First we measure the PEEM signal from our sample, which allows us to extract the XLD. We then measure the temperature dependence of the dichroism to separate the contributions from the magnetic and ferroelectric ordering. Finally, we switch the ferroelectric polarization using PFM, and record the effect on the dichroism; from this we extract the effect on the antiferromagnetic ordering of switching the ferroelectric polarization.

The XLD, which we image using PEEM[24,28], can have two possible origins. In non-ferroelectric antiferromagnets, such as $LaFeO_3$ or α-Fe_2O_3, asymmetry of the electronic charge distribution due to magnetic order causes a difference in the optical absorption between orthogonal linear polarizations of light[23,24,28–30]. This is manifested as a dichroism in the X-ray absorption, which can be used to distinguish different orientations of antiferromagnetic domains. The magnitude of this magnetic dichroism scales with the average of the square of the magnetic order parameter, as a result it is sensitive to the axis of magnetization (but not the direction) and reduces to zero at and above the Néel temperature. Non-magnetic ferroelectrics also show linear dichroism because their ferroelectricity causes an asymmetric electronic charge distribution. Therefore, in a magnetic ferroelectric such as $BiFeO_3$, both the antiferromagnetic ordering and the ferroelectric ordering can contribute to the dichroism, with the magnitude of the dichroism determined by the relative strengths of the two contributions, and the relative orientations of the antiferromagnetic and ferroelectric domains. The spatial resolution of the PEEM technique is around 50–100 nm; see refs 28, 29 for details.

Figure 3a,b shows PEEM images of the same region of the $BiFeO_3$ film, with the sample in Fig. 3b rotated in-plane by 90° relative to Fig. 3a. Note that we took a series of PEEM images at different X-ray photon energies around the Fe L_3 edge, and found that the linear dichroism has opposite values at the two L_3 absorption peak positions as in the structurally similar antiferromagnets hematite and lanthanum ferrite[28,30]. All the PEEM images shown in this paper are obtained by dividing the image intensity at each data point for the first L_3 peak by the corresponding intensity at the second peak. We define the linear dichroism value as the difference in intensity between the dark- and bright-tone regions in the PEEM images. It is clear that rotating in-plane by 90° causes a reversal of image contrast; this can be seen clearly in the finger-like patterns at the centre of the images. This reversal confirms that the PEEM signal is due to dichroism rather than an artefact of surface charge distribution[31], because any dichroism that results from non-uniformity in surface charge is independent of the X-ray polarization direction and photon energy. Figure 3c,d shows in-plane PFM images[26,27] of the same region of the film, again with the sample in Fig. 3d rotated in plane by 90° relative to Fig. 3c. There are two points to note. First, as in the PEEM case, rotation by 90° causes a reversal of image contrast. Second, the PEEM and in-plane PFM images are essentially identical. Therefore, the ferroelectric domain structure imaged using PFM correlates with the dichroism structure imaged using PEEM.

Next we separate out the relative contributions of the antiferromagnetic and ferroelectric domains to the dichroism, using temperature-dependent measurements[28,32] of the XLD from room temperature to 800 K. On heating, the antiferromagnetic contribution to the dichroism must reduce to zero at the Néel temperature (~640 K), whereas the ferroelectric contribution can persist up to the ferroelectric Curie temperature (~1,100 K).

In Fig. 4 we show our measured results for five samples; numbers 1–3 were recorded during heating, whereas 4 and 5 were recorded during cooling. In all cases the PEEM images were

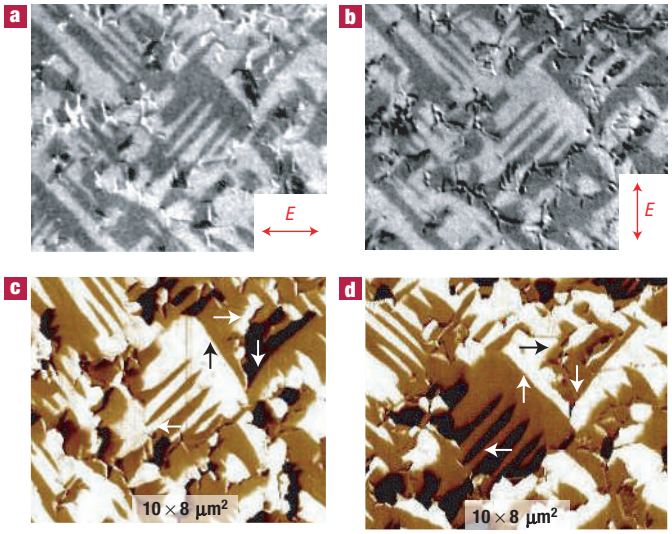

Figure 3 PEEM and in-plane PFM images taken in the same area of an as-grown $BiFeO_3$ film. a,**b**, PEEM images before (**a**) and after (**b**) 90° in-plane rotation between the two images. The arrows show the direction of X-ray polarization relative to the domain structure. **c**,**d**, In-plane PFM images before (**c**) and after (**d**) 90° in-plane rotation. The arrows show the direction of the in-plane component of ferroelectric polarization.

captured from the same area of the $BiFeO_3$ film after waiting 30 min at each temperature to allow thermal equilibration. The data in sample 2 were recorded on an electrically switched area (see later discussion), whereas the others were recorded on unswitched areas. We see that in all cases the linear dichroism signal drops rapidly on heating above room temperature, with only ~50% of the room-temperature XLD value remaining at the Néel temperature; this reduction is recovered on cooling. The XLD scales with $\langle M^2 \rangle$, the thermal average of the antiferromagnetic order parameter as shown in Fig. 4 (see refs 23,28 for details on calculating $\langle M^2 \rangle$). The XLD data in Fig. 4 closely follow this curve up to the Néel temperature. The XLD signal does not change significantly between the Néel temperature and 800 K. It is known in bulk BFO that the order parameter for ferroelectricity does not change much below its Curie temperature (~1,100 K), which is illustrated by the plots of Fe and Bi ionic displacements (from ref. 13) in Fig. 4. To investigate the ferroelectric order parameter in the 600 nm BFO film, we also plot the temperature-dependent out-of-plane lattice parameter obtained from X-ray diffraction, and the ferroelectric polarization obtained using high-frequency ferroelectric pulse measurements. Similar to bulk BFO, the 600 nm BFO film shows very little change in the ferroelectric order parameter from room temperature to 800 K and the order parameter change correlates with the high-temperature XLD signal. A PFM measurement also confirmed the existence of stable ferroelectricity in the BFO film up to 800 K (data not shown here). The bulk-like behaviour of the order parameter is consistent with earlier first-principles computations[33,34] and with the fact that minimal lattice strain is expected in the 600 nm film[20]. We therefore conclude that the high-temperature XLD signal results from the ferroelectric ordering, and the signal below T_N from the sum of the antiferromagnetic and ferroelectric contributions. At room temperature, the magnetic and ferroelectric components are of roughly equal strength and have the same sign.

We now turn to the question of whether ferroelectric polarization switching/rotation can switch the antiferromagnetic domain through the coupling of both order parameters to the ferroelastic domain structure, as outlined in the beginning of this paper. Figure 5a,b shows our PEEM results for the $BiFeO_3$ film before and after electrical poling, with the corresponding

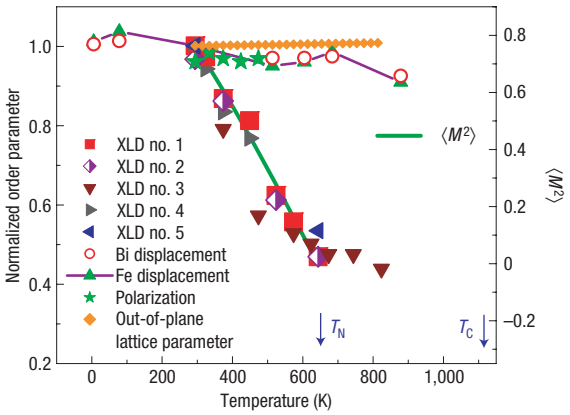

Figure 4 Temperature dependence of normalized order parameters of $BiFeO_3$. The linear dichroism, out-of-plane lattice parameter and ferroelectric polarization are normalized to the values at room temperature; the Bi and Fe atom displacements and $\langle M^2 \rangle$ are normalized to the values at 0 K.

in-plane PFM results shown in Fig. 5c,d. The poled area is outlined by dotted boxes in each figure. We know from the out-of-plane PFM images (not shown) that ferroelectric polarization switched under the applied bias, that is, −12 V. To unambiguously identify the polarization direction in each domain, in-plane PFM scans have been taken along two orthogonal ⟨110⟩ directions (only one shown here). The different switching mechanisms were easily distinguished by superimposing the in-plane PFM images taken before (the greyscale image) and after (the coloured image) electrical poling along the same direction, as shown in Fig. 5e. Owing to the image distortions associated with the inherent drifts in contact-mode imaging, the match is not perfect. The three possible switching mechanisms appear with different colours as marked in Fig. 5e. This image serves as a guide to identifying regions that exhibit different switching mechanisms in Fig. 5a–d. For example, regions 1 and 2 correspond to 109° switching, region 3

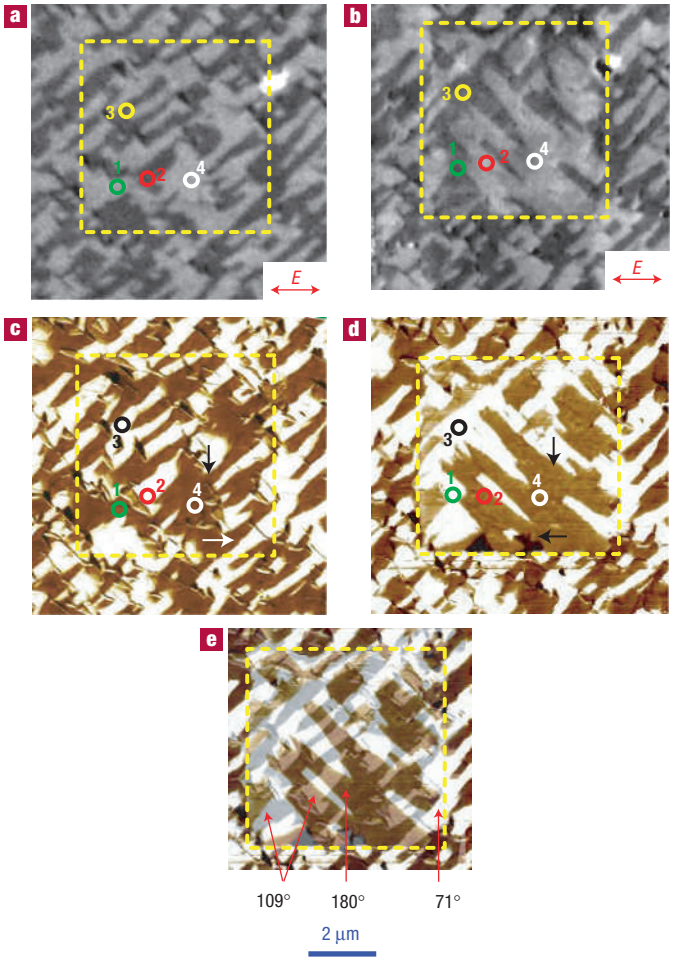

Figure 5 PEEM and in-plane PFM images of the same area of a $BiFeO_3$ film before and after electrical poling. a,**b**, PEEM images before (**a**) and after (**b**) poling. The arrows show the X-ray polarization direction during the measurements. **c**,**d**, In-plane PFM images before (**c**) and after (**d**) poling. The arrows show the direction of the in-plane component of ferroelectric polarization. Regions 1 and 2 (marked with green and red circles, respectively) correspond to 109° ferroelectric switching, whereas 3 (black and yellow circles) and 4 (white circles) correspond to 71° and 180° switching, respectively. In regions 1 and 2 the PEEM contrast reverses after electrical poling. **e**, A superposition of in-plane PFM scans shown in **c** and **d** used to identify the different switching mechanisms that appear with different colours and are labelled in the figure.

to 71° switching, and region 4 to 180° switching. Both 71° and 180° ferroelectric switching do not change the in-plane projection of the ferroelectric and antiferromagnetic order parameters (Fig. 1b,d), and thus cannot be detected by the current PEEM setup with a fixed X-ray polarization direction parallel to the sample surface. As a result, there is no observable contrast change in regions 3 and 4, although switching might have occurred. (Note that the discussion later will show that the ferroelectric and antiferromagnetic coupling in the 71° ferroelectric switching region might have a complicated behaviour. The PEEM results at least confirm that the in-plane projection of the antiferromagnetic axis is not changed by the 71° ferroelectric switching.) Our following discussion will focus on the regions with 109° ferroelectric switching.

As can be seen in Fig. 5, the PEEM images from the same area track the changes in the PFM images in the region with 109° ferroelectric switching: the PEEM contrast reverses, either from bright to dark (for example, region 1) or vice versa (for example, region 2), on ferroelectric switching. The expected PFM and PEEM contrast changes under the current experimental condition after ferroelectric polarization switching are summarized in Tables 1 and 2. Finally, we note that the dichroism value (that is the difference in intensity between the dark and bright domains) and temperature dependence are unchanged by the electrical switching, confirming that the antiferromagnetic domains are switching with the ferroelectric domains. (If the ferroelectric polarization switched without reorienting the antiferromagnetic axis, then the

Table 1 PFM contrast change after ferroelectric polarization switching.

Switching mechanism	PFM with cantilever along ⟨110⟩	
	In-plane	Out-of-plane
71°	Unchanged light* Unchanged dark Unchanged white	White ↔ dark
109°	Light ↔ white Light ↔ dark	White ↔ dark
180°	Unchanged light* White ↔ dark	White ↔ dark

* Indiscernible without sample rotation.

Table 2 Expected X-ray magnetic linear dichroism (XMLD)–PEEM contrast change after ferroelectric polarization switching.

Switching mechanism	XMLD–PEEM with X-ray E vector along ⟨110⟩ (image at the first L_3 peak/image at the second L_3 peak)
71°	Unchanged bright Unchanged dark
109°	Bright ↔ dark
180°	Unchanged bright Unchanged dark

ferroelectric component of the XLD would change sign, whereas the antiferromagnetic component would not. As a result, the dichroism value in the switched area would have a smaller value and a different temperature dependence.) Pioneered by Ascher and co-workers on Boracite[7] in 1960s, electric control of a magnetic domain has been reported on several materials, including $YMnO_3$ (ref. 4). The current result, however, goes further than the earlier work because it is (1) at room temperature; (2) on thin films, which is more favourable for applications; and (3) with an active control unlike in the $YMnO_3$ case[4]. To our knowledge, this is the first observation of ferroelectrically induced antiferromagnetic switching at room temperature. Very recently, an exchange bias coupling between an antiferromagnetic $BiFeO_3$ layer and an adjacent ferromagnetic layer has been reported[16]. By combining the ability to ferroelectrically control antiferromagnetism (as revealed in this work) and the ability of antiferromagnetic modulation of ferromagnetism[16], an ultimate electric control of ferromagnetism can be achieved.

We now recall that the first-principles calculation of the magnetocrystalline anisotropy in bulk $BiFeO_3$ predicted a sixfold degeneracy of the orientation of the antiferromagnetic sublattice magnetization within the (111) plane[21]. In such a case we would, in principle, expect to see many different antiferromagnetic domains within each ferroelectric domain with different projections of the antiferromagnetic order parameter on the polarization direction of the X-ray beam. However, in the PEEM measurements it seems that every ferroelectric domain coincides with only one antiferromagnetic domain. This could either mean that the sixfold degeneracy is broken in the films so that only one possible orientation of the antiferromagnetic axis with respect to the ferroelectric polarization occurs, or that we see only an 'effective' projection of the antiferromagnetic axis, averaged over all six possible orientations because of the resolution limits of the PEEM. The sixfold degeneracy could be lifted, for example, by a small monoclinic strain, which could indeed occur in a $BiFeO_3$ film grown on a (001) substrate; although the homogeneous strain in the 600-nm-thick films used in our experiments seems to be fully relaxed, a small inhomogeneous strain component could nevertheless still persist. Furthermore, the degeneracy of the magnetization direction could also be lifted by other effects related to the presence of the surface and the substrate. The discussion of the coupling between ferroelectric and antiferromagnetic switching presented in the next paragraph is basically independent of the precise mechanism behind the symmetry breaking.

We now investigate the effect of a small monoclinic strain on the easy magnetization direction by carrying out first-principles calculations of the magnetocrystalline anisotropy of $BiFeO_3$, analogous to the calculations of ref. 21, but with a slight monoclinic distortion of the unit cell vectors. After relaxation of all ions within the distorted unit cell, we calculate the relative energies for different orientations of the antiferromagnetic axis. As a result of the monoclinic distortion, the degeneracy is lifted and we find that an orientation of the antiferromagnetic axis parallel to the $[1\bar{1}0]$ direction is preferred, that is, perpendicular to the rhombohedral axis but simultaneously parallel to the (001) plane. As the $[1\bar{1}0]$ direction is perpendicular to both the [111] and $[11\bar{1}]$ directions, but not perpendicular to $[\bar{1}1\bar{1}]$, in this case we would expect the antiferromagnetic axis to rotate by 90° for the ferroelectric 109° switching and to be preserved during the 71° switching. The observed change in XLD contrast in the case of ferroelectric 109° switching is consistent with this scenario, although further experiments are required to fully establish the exact coupling scheme. In particular, an exact experimental determination of the orientation of the antiferromagnetic axis within the observed domains, for example, through an XLD-based PEEM measurement with different X-ray polarization directions, would provide valuable further insight. A setup that will facilitate such experiments is currently under construction at the Advanced Light Source.

Finally, we point out that the weak ferromagnetic magnetization in $BiFeO_3$ is perpendicular to both the ferroelectric polarization and the antiferromagnetic axes[21]. Therefore, similar switching effects can be expected for the weak magnetic moment, although the experimental observation might be even more difficult due to the small size of the corresponding order parameter. In particular, the 'reorientation behaviour' of the ferromagnetic moment is complementary to the behaviour of the antiferromagnetic axis, that is, if the antiferromagnetic axis is oriented along $[1\bar{1}0]$ (or equivalent directions) the ferromagnetic moment is along the $[11\bar{2}]$ direction, and is expected to reorient in the case of the 71° switching and to be preserved during the 109° switching.

In summary, we have observed a coupling between ferroelectricity and antiferromagnetism in $BiFeO_3$ thin films, which can be understood to result from the coupling of both antiferromagnetic and ferroelectric domains to the underlying ferroelastic domain structure. Such a coupling is a crucial first step in the exploration of approaches to control and switch magnetic properties using an electric field.

Received 22 May 2006; accepted 27 July 2006; published 3 September 2006.

References

1. Fiebig, M. Revival of the magnetoelectric effect. *J. Phys. D* **38,** R123–R152 (2005).
2. Spaldin, N. A. & Fiebig, M. The renaissance of magnetoelectric multiferroics. *Science* **309,** 391–392 (2005).
3. Eerenstein, W., Mathur, N. D. & Scott, J. F. Multiferroic and magnetoelectric materials. *Nature* **442,** 759–765 (2006).
4. Fiebig, M., Lottermoser, Th., Fröhlich, D., Goltsev, A. V. & Pisarev, R. V. Observation of coupled magnetic and electric domains. *Nature* **419,** 818–820 (2002).
5. Lottermoser, Th. *et al.* Magnetic phase control by an electric field. *Nature* **430,** 541–544 (2004).
6. Nan, C. W., Liu, G., Liu, Y. & Chen, H. Magnetic-field-induced electric polarization in multiferroic nanostructures. *Phys. Rev. Lett.* **94,** 197203 (2005).
7. Ascher, E., Rieder, H., Schmid, H. & Stössel, H. Some properties of ferromagnetoelectric nickel-iodine boracite, $Ni_3B_7O_{13}I$. *J. Appl. Phys.* **37,** 1404–1405 (1966).
8. Shastry, S., Srinivasan, G., Bichurin, M. I., Petrov, V. M. & Tatarenko, A. S. Microwave magnetoelectric effects in single crystal bilayers of yttrium iron garnet and lead magnesium niobate-lead titanate. *Phys. Rev. B* **70,** 064416 (2004).
9. Zheng, H. *et al.* Multiferroic $BaTiO_3$-$CoFe_2O_4$ nanostructures. *Science* **303,** 661–663 (2004).
10. Hill, N. A. Why are there so few magnetic ferroelectrics. *J. Phys. Chem.* **104,** 6694–6709 (2000).
11. Kimura, T., Lawes, G. & Ramirez, A. P. Electric polarization rotation in a hexaferrite with long-wavelength magnetic structures. *Phys. Rev. Lett.* **94,** 137201 (2005).
12. Kubel, F. & Schimid, H. Structure of a ferroelectric and ferroelastic monodomain crystal of the perovskite $BiFeO_3$. *Acta Crystallogr. B* **46,** 698–702 (1990).
13. Fischer, P., Polomska, M., Sosnowska, I. & Szymanski, M. Temperature dependence of the crystal and magnetic structure of $BiFeO_3$. *J. Phys. Solid State Phys.* **13,** 1931–1940 (1980).
14. Michel, C., Moreau, J.-M., Achenbach, G. D., Gerson, R. & James, W. J. The atomic structure of $BiFeO_3$. *Solid State Commun.* **7,** 701–704 (1969).
15. Wang, J. *et al.* Epitaxial $BiFeO_3$ multiferroic thin film heterostructures. *Science* **299,** 1719–1722 (2003).
16. Dho, J., Qi, X., Kim, H., MacManus-Driscoll, J. L. & Blamire, M. G. Large electric polarization and exchange bias in multiferroic $BiFeO_3$. *Adv. Mater.* **18,** 1445–1448 (2006).
17. Li, J. F. *et al.* Dramatically enhanced polarization in (001), (101), and (111) $BiFeO_3$ thin films due to epitiaxial-induced transitions. *Appl. Phys. Lett.* **84,** 5261–5263 (2004).
18. Yun, K. Y. *et al.* Structural and multiferroic properties of $BiFeO_3$ thin films at room temperature. *J. Appl. Phys.* **96,** 3399–3403 (2004).
19. Yun, K. Y., Noda, M. & Okuyama, M. Prominent ferroelectricity of $BiFeO_3$ thin films prepared by pulsed-laser deposition. *Appl. Phys. Lett.* **83,** 3981–3983 (2003).

20. Das, R. R. *et al.* Synthesis and ferroelectric properties of epitaxial $BiFeO_3$ thin films grown by sputtering. *Appl. Phys. Lett.* **88,** 242904 (2006).
21. Ederer, C. & Spaldin, N. A. Weak ferromagnetism and magnetoelectric coupling in bismuth ferrite. *Phys. Rev. B* **71,** 060401(R) (2005).
22. Neaton, J. B., Ederer, C., Waghmare, U. V., Spaldin, N. A. & Rabe, K. M. First-principles study of spontaneous polarization in multiferroic $BiFeO_3$. *Phys. Rev. B* **71,** 014113 (2005).
23. Thole, B. T., van der Laan, G. & Sawatzky, G. A. Strong magnetic dichroism predicted in the $M_{4,5}$ X-ray absorption spectra of magnetic rare-earth materials. *Phys. Rev. Lett.* **55,** 2086–2088 (1985).
24. Czekaj, S., Nolting, F., Heyderman, L. J., Willmott, P. R. & van der Laan, G. Sign dependence of the X-ray magnetic linear dichroism on the antiferromagnetic spin axis in $LaFeO_3$ thin films. *Phys. Rev. B* **73,** 020401(R) (2006).
25. Bai, F. *et al.* Destruction of spin cycloid in $(111)_c$-oriented $BiFeO_3$ thin films by epitaxial constraint: Enhanced polarization and release of latent magnetization. *Appl. Phys. Lett.* **86,** 032511 (2005).
26. Zavaliche, F. *et al.* Ferroelectric domain structure in epitaxial $BiFeO_3$ films. *Appl. Phys. Lett.* **87,** 182912 (2005).
27. Zavaliche, F. *et al.* Polarization switching in epitaxial $BiFeO_3$ films. *Appl. Phys. Lett.* **87,** 252902 (2005).
28. Scholl, A. *et al.* Observation of antiferromagnetic domains in epitaxial thin films. *Science* **287,** 1014–1016 (2000).
29. Scholl, A., Ohldag, H., Nolting, F., Stöhr, J. & Padmore, H. A. X-ray photoemission electron microscopy, a tool for the investigation of complex magnetic structures (invited). *Rev. Sci. Instrum.* **73,** 1362–1366 (2002).
30. Luning, J. *et al.* Determination of the antiferromagnetic spin axis in epitaxial $LaFeO_3$ films by x-ray magnetic linear dichroism spectroscopy. *Phys. Rev. B* **67,** 214433 (2003).
31. Yang, W. C., Rodriguez, B. J., Gruverman, A. & Nemanich, R. J. Polarization-dependent electron affinity of $LiNbO_3$ surfaces. *Appl. Phys. Lett.* **85,** 2316–2318 (2004).
32. Tsuboi, T. Linear dichroism study of the structural phase transition of $BaMnF_4$. *Phys. Rev. B* **39,** 2842–2845 (1989).
33. Ederer, C. & Spaldin, N. Effect of epitaxial strain on the spontaneous polarization of thin film ferroelectrics. *Phys. Rev. Lett.* **95,** 257601 (2005).
34. Ederer, C. & Spaldin, N. Influence of strain and oxygen vacancies on the magnetoelectric properties of multiferroic bismuth ferrite. *Phys. Rev. B* **95,** 224103 (2005).

Acknowledgements

This work is supported by an ONR grant No. N00014-06-1-0008, N00014-05-1-0559 (CBE) monitored by Colin Wood and an ONR-MURI grant No. E-21-6RU-G4. This work was also supported by the National Science Foundation under grants DMR-0313764 (CBE) and ECS-0210449 (CBE) and a David & Lucile Packard Fellowship (CBE). Partial support from a LBL LDRD and a MARCO program is also gratefully acknowledged. C.E. and N.A.S. are supported by the NSF's 'Chemical Bonding Centers' program, grant No. CHE-0434567 and made use of the central facilities provided by the NSF-MRSEC Award No. DMR05-20415.
Correspondence and requests for materials should be addressed to T.Z. or R.R.

Competing financial interests

The authors declare that they have no competing financial interests.